Received: 19 May 2021 | Revised: 30 June 2021 | Accepted: 18 July 2021

DOI: 10.1002/jmor.21400

RESEARCH ARTICLE

morphology WILEY

Evaluating bony predictors of bite force across the order Carnivora

Edwin Dickinson[1] | Jillian S. Davis[2] | Ashley R. Deutsch[1] | Dhuru Patel[1] | Akash Nijhawan[1] | Meet Patel[1] | Abby Blume[1] | Jordan L. Gannon[3] | Cassandra M. Turcotte[4,5] | Christopher S. Walker[6] | Adam Hartstone-Rose[1]

[1]Department of Biological Sciences, North Carolina State University, Raleigh, North Carolina, USA

[2]Pathology, Anatomy, and Laboratory Medicine Department, West Virginia University School of Medicine, Morgantown, West Virginia, USA

[3]Biology Department, High Point University, High Point, North Carolina, USA

[4]Department of Anthropology, New York University, New York, New York, USA

[5]New York Consortium in Evolutionary Primatology, New York, New York, USA

[6]Department of Molecular Biomedical Sciences, North Carolina State University, Raleigh, North Carolina, USA

Correspondence
Adam Hartstone-Rose, Department of Biological Sciences, North Carolina State University, Raleigh, NC, USA.
Email: adamhrose@ncsu.edu

Funding information
Division of Behavioral and Cognitive Sciences, Grant/Award Number: 14-40599; Division of Integrative Organismal Systems, Grant/Award Number: 15-57125

Abstract

In carnivorans, bite force is a critical and ecologically informative variable that has been correlated with multiple morphological, behavioral, and environmental attributes. Whereas in vivo measures of biting performance are difficult to obtain in many taxa—and impossible in extinct species—numerous osteological proxies exist for estimating masticatory muscle size and force. These proxies include both volumetric approximations of muscle dimensions and direct measurements of muscular attachment sites. In this study, we compare three cranial osteological techniques for estimating muscle size (including 2D-photographic and 3D-surface data approaches) against dissection-derived muscle weights and physiological cross-sectional area (PCSA) within the jaw adductor musculature of 40 carnivoran taxa spanning eight families, four orders of magnitude in body size, and the full dietary spectrum of the order. Our results indicate that 3D-approaches provide more accurate estimates of muscle size than do surfaces measured from 2D-lateral photographs. However, estimates of a muscle's maximum cross-sectional area are more closely correlated with muscle mass and PCSA than any estimates derived from muscle attachment areas. These findings highlight the importance of accounting for muscle thickness in osteological estimations of the masticatory musculature; as muscles become volumetrically larger, their larger cross-sectional area does not appear to be associated with a proportional increase in the attachment site area. Though volumetric approaches approximate muscle dimensions well across the order as a whole, caution should be exercised when applying any single method as a predictor across diverse phylogenies.

KEYWORDS
bony correlates, entheses, masseter, PCSA, temporalis

1 | INTRODUCTION

A mammal's feeding system is shaped by the need to consume sufficient resources from its environment to satisfy metabolic demands. Within this paradigm, bite force influences dietary choice by constraining the upper limits of mechanical resistance for potential foods. Scaling trends in bite force, therefore, provide valuable insight into dietary ecology across a lineage, and a crucial lens to understanding functional adaptation across ecologically diverse families and/or orders. The order Carnivora is the most ecomorphologically diverse among mammals (Christiansen & Wroe, 2007; Nowak, 1991), with terrestrial species alone spanning four orders of magnitude in body

size (from 60–100 g in *Mustela nivalis* to >500 kg in *Ursus arctos* and *U. maritimus*) and encompassing a broad dietary spectrum ranging from hypercarnivory to obligate durophagous folivory. Consequently, many studies have sought to estimate and compare bite force across this order (Christiansen & Adolfssen, 2005; Christiansen & Wroe, 2007; Hartstone-Rose et al., 2012; Hartstone-Rose et al., 2019; Penrose et al., 2020; Radinsky, 1981a; Radinsky, 1981b; Wroe et al., 2005). Such analyses have suggested several overarching trends, such as relatively high bite force within felids and mustelids compared to canids and ursids (Radinsky, 1981a; Radinsky, 1981b), which may reflect an increased reliance upon carnivory within the former families and a greater frequency of omnivory in the latter. Indeed, a reanalysis of this hypothesis (Christiansen & Wroe, 2007) reports that, across the order as a whole, large-prey consuming carnivores and durophagous taxa are associated with high relative bite forces, while omnivores and small-prey specialists have relatively reduced bite forces when adjusted for body mass. This relationship between dietary ecology and bite force within the Carnivora offers significant potential to paleontological studies of dietary niche diversification. However, before these methods are applied to the reconstruction of myology in fossils, it is imperative to the first evaluate the efficacy of these osteological estimates in predicting myology of modern species, and to determine which reconstruction approaches offer the greatest accuracy.

1.1 | Estimating bite force

Previous attempts to quantify bite force in extant species have employed a broad array of methodologies. Among these, the most straightforward is the use of a bite force transducer, which is placed at a specified bite point in the mouth and registers contact forces during the biting motion. Through this technique, in vivo bite force data are reported for a number of mammalian taxa (e.g., see Aguirre et al., 2002; Becerra et al., 2011; Becerra et al., 2014; Binder & Van Valkenburgh, 2000; Brassard et al., 2020; Brassard et al., 2021; Dechow & Carlson, 1990; Dumont et al., 2009; Santana & Dumont, 2009; Williams et al., 2009) as well as a plethora of lizards (e.g., Gröning et al., 2013; Herrel, Damme, et al., 2001; Herrel, De Grauw, & Lemos-Espinal, 2001; Herrel & O'Reilly, 2006; Meyers et al., 2002; Ross et al., 2018). However, data on Carnivora, particularly among larger-bodied animals, are sparse. As a direct measurement technique, in vivo bite force data requires access to specimens and approval for measurements, which renders it complex (and often impossible) to accumulate comparative data across large numbers of focal taxa. Moreover, it is possible that voluntary bite forces collected in this way may be influenced by many confounding environmental variables (such as the animal's familiarity with handling, current disposition, and general stress levels) such that the forces measured may not closely correspond to the animal's true maximal or habitual bite forces (as discussed in, e.g., Davis et al., 2010, Becerra et al., 2014).

Bite force can also be approximated cadaverically using anatomical correlates (e.g., Hartstone-Rose et al., 2012; Hartstone-Rose et al., 2019). As the size and internal configuration of muscles determine their contractile properties, dissection of the jaw-adductor musculature permits bite force to be estimated myologically. Skeletal muscle consists of individual fibers, which are themselves comprised of serially arranged sarcomeres: the motor units of muscle tissue which contract simultaneously to produce force (Gans, 1982; Gans & Bock, 1965). By increasing total fiber count (either by shortening fibers to permit a greater number to be accommodated within a given volume or by increasing the overall volume of muscle tissue), contractile force potential is also increased (Gans, 1982; Lieber, 1986; Lieber & Fridén, 2000). The magnitude of force a muscle may produce is calculated by a muscle's physiological cross-sectional area (PCSA), which is derived by combining muscle mass, fiber lengths, and muscle density. PCSA has been experimentally demonstrated to be proportional to force generation potential (Powell et al., 1984) when translated using a force constant which typically ranges from 24 to 32 N/cm^2. While this technique circumvents the requirement for in vivo animal experimentation, it is instead reliant upon access to fresh or well-preserved cadaveric specimens for all focal taxa, a demand which is often difficult to satisfy, and relies on other assumptions like the maximal simultaneous contraction of all fascicles during a bite.

Both in vivo and muscle-based methods of estimating bite force are inherently applicable only to extant taxa for which living or recently deceased specimens are available. By comparison, osteological techniques for estimating muscle volume (which then serve as a proxy for force potential) permit the inclusion of fossil specimens for which the cranium and/or mandible are suitably preserved, while similarly enhancing potential taxonomic diversity within comparative studies of extant taxa.

Several techniques have been proposed for the estimation of masticatory muscle size from bone (Figure 1). Among these, the most frequently used in recent studies of the carnivoran skull is the "dry-skull" method proposed by Thomason (1991), which uses a pair of 2D cross-sectional areas as a proxy for masticatory muscle size (Figure 1c,d). The first measurement, used to approximate the temporalis, is measured as a cross-sectional slice bound laterally by the zygomatic arch, medially by the neurocranium, posteriorly by the zygomatic root, and anteriorly by the postorbital process with the skull aligned in a posterodorsal view to place the zygomatic root and the postorbital process into a parallel plane (Figure 1c). The second measurement, which estimates the size of the masseter (and also ostensibly the medial pterygoid, though practically no measurements that account for variation in this muscle are included) is measured as a cross-sectional area defined as the area contained by the zygomatic arch with the skull in an inferior configuration (Figure 1d). These areas are then treated similarly to PCSA, being multiplied by a force constant to translate into bite force potential.

Thomason's proxy for muscle size was initially validated on a small interspecific sample of seven taxa across a number of mammalian orders and ranges of body size. Log–log regressions suggest a close correlation between myologically-derived and osteologically predicted muscle masses and PCSA ($r = .99$). This technique has subsequently

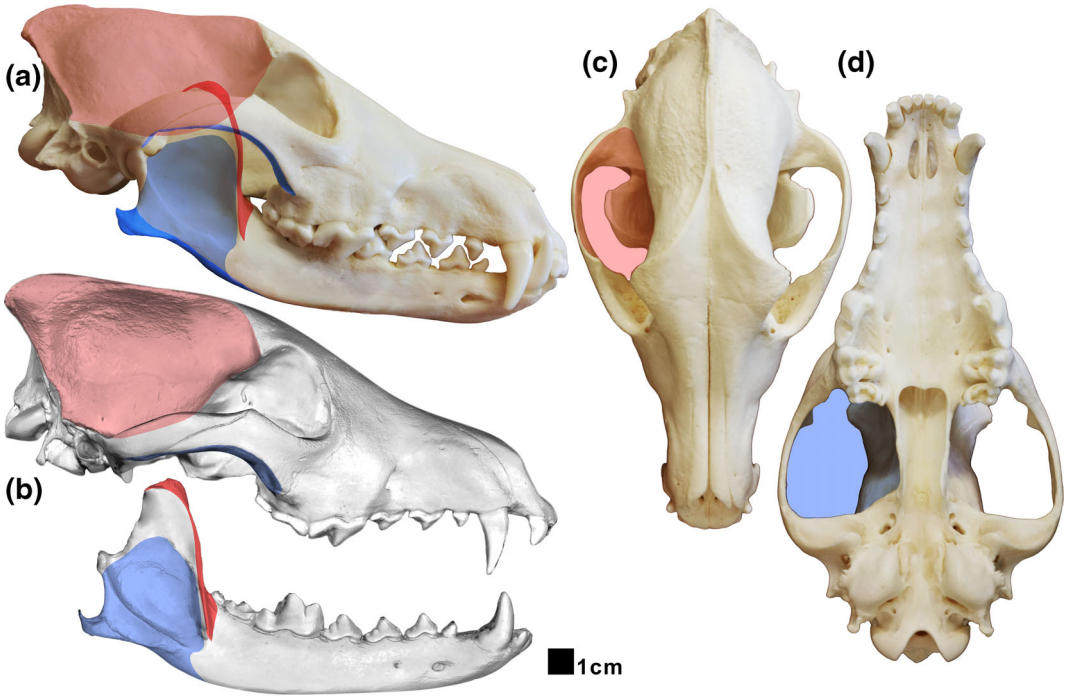

FIGURE 1 Methodology for quantifying osteological proxies of muscle size. (a) 2D muscle attachment areas measured from craniomandibular lateral photograph; (b) 3D muscle attachment areas measured from digitized crania and mandibles; Thomason "dry skull" technique for estimating temporalis (c) and masseter (d) cross-section. Red = surface areas for attachments (a and b) or cross-section (c) of temporalis; blue = surface areas for attachments (a and b) or cross-section (d) of masseter. Masseter insertion was measured two ways in the lateral photograph method (a)—(1) SM + DM + ZM approach of the whole muscle attachment (including the insertion of zygomaticomandibularis in the whole masseteric fossa, shown by dark and light blue combined) and (2) the SM + DM approach that isolated the insertion areas of the superficial and deep masseter only (dark blue only)

been used in several prominent studies of osteological bite force reconstruction (Christiansen & Adolfssen, 2005; Christiansen & Wroe, 2007; Forbes-Harper et al., 2017; Wroe et al., 2005). More recently still, attempts have been made to further validate this technique, yielding mixed results. In vivo bite force data collected on *Didelphis virginiana* correspond well with Thomason's original osteological estimates of bite force within this taxon (Law et al., 2018). However, evaluations of this technique on more taxonomically diverse samples have yielded poorer results; within the Phyllostomidae, for example, the technique was found to consistently overpredict cross-sectional area within the masseter-pterygoid complex while underpredicting the cross-sectional area of the temporalis (Davis et al., 2010).

Several other techniques have relied on more direct bony proxies for muscle size, using either attachment site scars on the zygomatic (Demes & Creel, 1988) or mandible (Emerson & Radinsky, 1980) as direct proxies for masseter size or combining multiple linear metrics to estimate cross-sectional area (Antón, 1994; Antón, 1999). Among these linear predictors, substantial variation in reliability is observed. While masseter origin and insertion site lengths show relatively strong correspondence between PCSA and predicted muscle CSA (r^2 = .69 and .73, respectively), other tested metrics such as "zygarea" (the product of masseter origin area length and zygomatic arch width) showed relatively little correlation with PCSA (r^2 = .38) across three species of *Macaca* (Antón, 1994).

Stronger correlates of muscle cross-sectional area appear to be found when quantifying the overall area of muscle attachment site instead of linear metrics of attachment site length/width. Using a broad sample of strepsirrhines, Perry et al. (2015) report strong correlations (r^2 = .81–.91) between 3D attachment surface areas of the masseter and temporalis and PCSA data of the equivalent muscles. Although measured by flattening physical 3D molds of these surface areas, the approach is fundamentally similar to measuring these surface areas in digital space (e.g., as in Figure 1b). Lateral photographs of the cranium and mandible have also been used to approximate the size and centroids of attachment areas for the jaw adductors of carnivorans and primates when calculating biomechanical leverages of the masticatory apparatus (Deutsch et al., 2020; Hartstone-Rose et al., 2012; Hartstone-Rose et al., 2019), as have morphometric approaches to the characterization of muscle attachment areas in 3D space (Fabre et al., 2018). However, questions remain as to how effectively these varying methods can predict myological parameters of the masticatory apparatus across anatomically and taxonomically diverse samples that spans major variation in both body size and craniomandibular form. Moreover, muscle attachment areas have been shown to be of varying value for predicting muscle size and strength within other skeletal regions. While correlations between muscle size/force and entheseal areas have been questioned in several postcranial regions (e.g., Turcotte et al., 2020; Wallace

et al., 2017; Zumwalt, 2006), some morphometric approaches have suggested a relationship between muscle force potential (i.e., PCSA) and external bony morphology (Harbers, Neaux, et al., 2020; Harbers, Zanolli, et al., 2020). Thus, the predictive value of muscle attachment sites for the estimation of myological properties remains contentious.

1.2 | Hypothesis and predictions

Within this study, we evaluate several methodologies for the osteological prediction of muscle mass and PCSA across a large and diverse carnivoran sample, designed to maximally incorporate the full range of body sizes, dietary niches, and morphological diversity encompassed by this order. Dissection-derived muscle masses and PCSA data for the temporalis and masseter of each taxon are compared to osteological predictions derived using three distinct techniques: evaluations of 2D attachment areas (Figure 1a), 3D attachment areas (Figure 1b), and the "dry-skull" cross-sectional estimation technique (Figure 1c) as described by Thomason (1991). In so doing, we test the overarching hypothesis that osteological correlates of the masticatory musculature can reliably predict bite force across the order Carnivora. To this end, we propose the following predictions:

1.2.1 | Prediction 1

Following recent studies that have highlighted shortcomings in the accuracy of the "dry skull" method within certain lineages (Davis et al., 2010) and the strong accordance between PCSA and 3D attachment areas demonstrated in strepsirrhines by Perry et al. (2015), we predict that metrics accounting directly for the muscle attachment areas (e.g., 2D and 3D origin and insertion areas) will be more strongly correlated with muscle mass and PCSA than the representative cross-sectional areas associated with the "dry skull" method.

1.2.2 | Prediction 2

Among estimates of surface attachment areas, the inclusion of the z-plane within our 3D data should improve the accuracy of myological predictions by accounting for the curvature of the bone (e.g., wrapping of the temporalis origination around the neurocranium). Thus, we predict that 3D attachments (measured from surface scans of each specimen) will more strongly correlate with muscle mass and PCSA than their 2D counterparts.

1.2.3 | Prediction 3

Among attachment areas, we anticipate variation in the accuracy of individual variables. Specifically, we predict that large, fleshy attachment areas (e.g., the origin of temporalis) will show a stronger correlation with muscle mass and PCSA than do tendinous attachments (e.g., the insertion of temporalis) as the former is more anatomically integrated with the body of the muscle.

1.2.4 | Prediction 4

As muscle mass is more closely associated with muscle volume than PCSA (which is additionally impacted by fascicle lengths), we predict that muscle mass will be universally more strongly correlated with bony metrics than is PCSA in all muscles.

1.2.5 | Prediction 5

Due to differences in cranial morphology, niche diversification, dietary variability, and body size range (particularly on the lower end of this range) between the suborders feliformia (families Felidae, Hyaenidae, and Herpestidae) and caniformia (families Canidae, Ursidae, Mustelidae, Mephitidae, and Procyonidae), we predict that the relationships between bony metrics and myological properties will differ between these two taxa. As feliforms are more ecomorphologically conservative, we predict that bony metrics will be more predictive across this suborder than in caniforms.

2 | MATERIALS AND METHODS

2.1 | Data acquisition

Myological and osteological data were collected for 40 specimens of Carnivora, representing eight families (Canidae, Felidae, Hyaenidae, Herpestidae, Mustelidae, Procyonidae, Mephitidae and Ursidae; see Table 1). All specimens represented skeletally mature adults and no specimens presented notable masticatory pathologies. All specimens were dissected freshly frozen, without formalin fixation or ethanol storage, with the exception of three taxa: *Crocuta crocuta* (AMNH 200618), *Helarctos malayanus* (USNM 257411), and *Nyctereutes procyonoides* (USNM 497835), which were sourced from museum collections (see details on fixation adjustment below). Dissection data were collected following a standardized sharp dissection protocol and include previously published data for felid, procyonid, mephitid, and mustelid specimens (Hartstone-Rose et al., 2012; Hartstone-Rose et al., 2019) and other carnivores dissected following the same methods for a paper predominantly on canids and ursids (Hartstone-Rose et al., in press). In brief, skin and overlying fascia were first removed to expose the underlying muscle tissue. Muscles were then excised individually and weighed to the nearest 0.0001 g using a Mettler-Toledo digital balance. Individual muscles were then submerged in either a 10% sulfuric acid solution at 60°C or a 35% nitric acid solution at room temperature until connective tissues were dissolved, following a modified protocol from Rayne and Crawford (1972). Muscles were then transferred into a 50% aqueous glycerol solution to prevent further digestion. Once stabilized in

TABLE 1 Study sample and muscle architectural data

Species name	Suborder	Taxonomic group	Specimen ID	BM (g)	Temporalis mass (g)	Masseter mass (g)	Temporalis PCSA (cm^2)	Masseter PCSA (cm^2)
Aonyx cinerea	Caniformia	Musteloid	AHR-213055	3100	12.54	3.15	0.93	0.24
Bassariscus astutus	Caniformia	Musteloid	AHR-211021	985	6.49	2.12	0.64	0.24
Canis latrans	Caniformia	Canid	AHR-208010	14,000	67.49	31.74	3.09	1.84
Canis lupus	Caniformia	Canid	AHR-208003	59,420	335.47	137.32	11.67	5.87
Canis rufus	Caniformia	Canid	AHR-208046	27,215	173.70	66.95	5.90	3.64
Caracal caracal	Feliformia	Felid	AHR-202029	16,590	51.91	35.53	2.71	2.57
Crocuta crocuta[a]	Feliformia	Hyenid	AHR-205003	68,000	415.48	98.21	19.28	6.50
Eira barbara	Caniformia	Musteloid	AHR-213050	4850	10.42	3.65	0.81	0.40
Felis nigripes	Feliformia	Felid	AHR-202111	1300	6.76	4.98	0.69	0.46
Gulo gulo	Caniformia	Musteloid	AHR-213006	18,143	128.13	30.09	6.03	2.00
Helarctos malayanus[a]	Caniformia	Ursid	AHR-209001	45,000	366.91	160.38	10.24	3.83
Herpestes javanicus	Caniformia	Musteloid	AHR-206007	2250	5.98	1.44	0.46	0.15
Leopardus pardalis	Feliformia	Felid	AHR-202059	11,590	54.46	35.32	3.31	2.50
Leptailurus serval	Feliformia	Felid	AHR-202103	13,900	44.01	29.07	3.77	1.87
Lontra canadensis	Caniformia	Musteloid	AHR-213051	9500	24.32	6.95	1.23	0.56
Lycaon pictus	Caniformia	Canid	AHR-208024	26,500	180.19	88.68	7.21	4.36
Lynx rufus	Feliformia	Felid	AHR-202067	15,500	29.67	24.25	1.87	1.79
Martes americana	Caniformia	Musteloid	AHR-213066	860	4.78	1.52	0.42	0.18
Mephitis mephitis	Caniformia	Musteloid	AHR-212007	3075.	9.70	2.40	1.04	1.21
Mustela erminea	Caniformia	Musteloid	AHR-213091	131	0.58	0.09	0.07	0.06
Nasua nasua	Caniformia	Musteloid	AHR-211040	4100	12.39	5.82	1.12	0.60
Neofelis nebulosa	Feliformia	Felid	AHR-202001	24,000	101.39	77.00	6.47	3.78
Neovison vison	Caniformia	Musteloid	AHR-213068	1148	3.15	0.69	0.24	0.11
Nyctereutes procyonoides[a]	Caniformia	Canid	AHR-208030	4424	42.93	20.62	1.76	1.08
Panthera onca	Feliformia	Felid	AHR-202023	100,000	502.00	268.28	20.34	12.15
Panthera pardus	Feliformia	Felid	AHR-202013	34,100	146.00	71.00	5.96	4.80
Panthera tigris	Feliformia	Felid	AHR-202107	200,000	921.00	503.00	27.48	19.91
Panthera uncia	Feliformia	Felid	AHR-202003	38,640	130.94	65.85	6.49	3.80
Potos flavus	Caniformia	Musteloid	AHR-211022	3000	8.55	3.10	0.71	0.36
Procyon lotor	Caniformia	Musteloid	AHR-211047	5940	19.89	8.40	1.20	0.79
Pteronura brasiliensis	Caniformia	Musteloid	AHR-213014	30,000	161.53	22.60	32.90	1.51
Spilogale putorius	Caniformia	Musteloid	AHR-212010	562	3.91	0.98	1.26	0.58
Suricata suricatta	Feliformia	Herpestid	AHR-206010	731	6.15	2.31	0.39	0.27
Taxidea taxus	Caniformia	Musteloid	AHR-213003	12,020	27.10	7.60	2.47	0.71
Tremarctos ornatus	Caniformia	Ursid	AHR-209012	83,940	189.73	83.63	6.54	3.62
Ursus americanus	Caniformia	Ursid	AHR-209004	113,398	260.68	62.22	8.57	3.40
Ursus arctos	Caniformia	Ursid	AHR-209015	389,000	902.00	239.00	28.29	8.74
Vulpes macrotis	Caniformia	Canid	AHR-208050	1900	8.47	2.45	0.64	0.12
Vulpes vulpes	Caniformia	Canid	AHR-208049	8500	25.17	7.60	1.33	0.70
Vulpes zerda	Caniformia	Canid	AHR-205040	969	4.77	2.06	0.34	0.23

[a]denotes specimen formalin-fixed and ethanol-stored prior to dissection, and thus corrected for muscle mass and density following Leonard, Worden, Boettcher, Dickinson, and Hartstone-Rose (2021) and Leonard, Worden, Boettcher, Dickinson, Omstead, et al. (2021). Body mass data derived from Wilson and Mittermeier (2009).

glycerol, individual muscle fascicles were manually separated using forceps and photographed alongside a scale bar. Fascicle lengths were then measured using the software package ImageJ v1.51 (Schneider et al., 2012). Phyiological cross sectional area (PCSA) was calculated by combining mass and fascicle length data using the formula

$$q = \frac{m}{lp}$$

taken from Schumacher (1961) in which q represents PCSA, m represents muscle mass (in grams), l represents the average fascicle length of each muscle, and p represents a constant defining the specific density of skeletal muscle. A density constant of 1.0606 g/cm^3 was applied to all specimens dissected as fresh tissue, following region-specific guidelines outlined by Leonard, Worden, Boettcher, Dickinson, Omstead, et al. (2021). For the three specimens formalin-fixed and ethanol-stored prior to dissection (*Crocuta crocuta*, *Helarctos malayanus*, and *Nyctereutes procyonoides*; Table 1), a density constant of 1.0033 was applied, following Leonard, Worden, Boettcher, Dickinson, and Hartstone-Rose (2021). In addition, a correction factor of 2.64x was applied to the muscle masses of these specimens to account for volumetric loss during fixation and long-term ethanol storage (Leonard, Worden, Boettcher, Dickinson, & Hartstone-Rose, 2021). These adjusted muscle densities and masses were then used in the calculation of PCSA, as above. (Leonard, Worden, Boettcher, Dickinson, & Hartstone-Rose, 2021, found that fascicles of muscles preserved on the bone were not significantly different in length from those measured fresh, and therefore only mass and density require correction in these museum specimens.)

Osteological photographs were taken of each taxon in three orientations using a Canon EOS 5DS. The first photo comprised an articulated cranium and mandible in lateral pose with the upper and lower dentition in full occlusion (Figure 1a). The second and third photographs followed the protocol of Thomason (1991), and featured the cranium aligned in a posterodorsal view to align the zygomatic root and the postorbital process in a plane parallel to the camera (Figure 1c) and the cranium in an inferior view (Figure 1d). Nineteen specimens utilized individually-matched myological and osteological data, while the remainder used sex-matched, representative osteological specimens. However, no impact of conspecificity was observed within our analysis. Each photograph was taken with a scale bar and subsequently imported into ImageJ wherein muscle attachment areas were outlined and measured (Figure 1).

Specimens were subsequently surface scanned using either a David SLS-3, HDI 120A-B, Faro ScanArm 3D-scanner, or Nikon XTH 225 ST μCT-scanner. In each instance, the cranium and mandible were scanned separately, and each element was scanned in multiple planes before scans were merged together to create a 3D-composite. Resultant scans were produced and standardized to ~2,000,000 triangles apiece, though large specimens (e.g., Ursidae, *Panthera*) produced larger models of ~5,000,000 triangles. From these scans, surface areas corresponding to regions of muscle attachment (that matched outlined surface areas from the lateral photographs outlined above) were isolated and extracted using Geomagic Wrap 2017 (Figure 1b). The external surface area of each muscle attachment site was then measured using the same software package. Finally, in one proxy (masseter 2D-insertion area), two different techniques for determining the attachment areas were used: one (SM + DM) using just the inferior borders of this muscle's attachment (i.e., insertion area of the superficial masseter and deep masseter; Figure 1a), and one (SM + DM + ZM) that incorporated the masseteric fossa (i.e., the above plus the insertion area of the zygomaticomandibularis; Figure 1a). Though the zygomaticomandibularis comprises only a small portion of the masseter by volume, its insertion area is large; thus, this comparison made it possible to examine the influence of including this region in the osteological prediction of masseter size and force. Surface scans of the specimens analyzed above can be found at https://www.morphosource.org/projects/000370762?locale=en

TABLE 2 Summary statistics following phylogenetic reduced major axis (RMA) regressions of bony correlate predictors against muscle mass

	Bony metric	Slope All carnivores	Intercept	R^2	Slope Caniformia	Intercept	R^2	Slope Feliformia	Intercept	R^2
Masseter	Thomason "dry skull"	0.89	1.18	.91*	0.86	1.19	.91*	0.94	1.15	.92
	2D origin	0.15	0.97	.89**	0.15	0.97	.88**	0.14	0.96	.92**
	2D insertion (SM + DM)	1.00	0.58	.78	1.07	0.59	.83	0.81	0.66	.79
	2D insertion (SM,DM,ZM)	0.99	1.07	.90	0.95	1.04	.90	1.11	0.91	.96
	3D origin	1.11	0.55	.75	1.15	0.53	.76	0.94	0.66	.81
	3D insertion	0.92	1.05	.90	0.86	1.08	.91*	1.10	0.94	.93
Temporalis	Thomason "dry skull"	1.09	0.85	.92	1.06	0.87	.91	1.15	0.81	.97*
	2D origin	0.75	1.24	.90**	0.77	1.23	.90**	0.73	1.24	.94**
	2D insertion	1.23	0.43	.78*	1.36	0.38	.74	0.96	0.66	.94
	3D origin	0.77	1.28	.90**	0.76	1.29	.89**	0.81	1.25	.94*
	3D insertion	1.09	0.30	.75	1.16	0.28	.75	0.89	0.43	.72

Note: Statistical significance is indicated by *p < .05 and **p < .01.

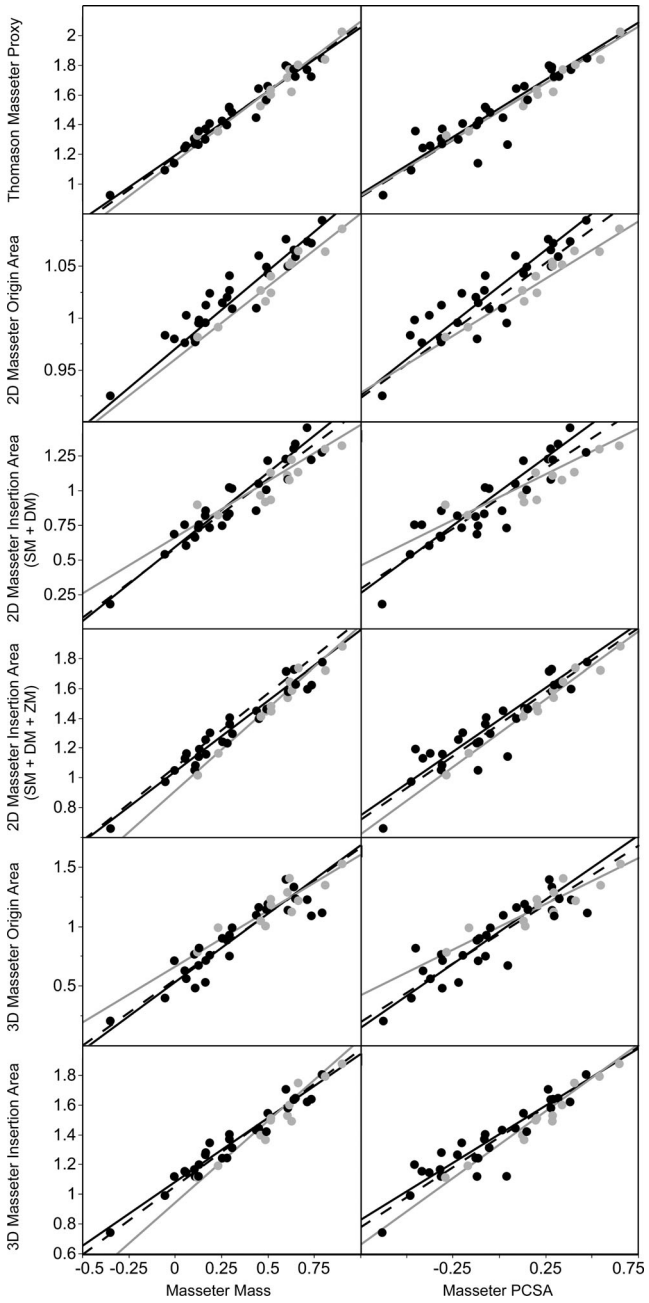

FIGURE 2 Reduced major axis (RMA) regressions of various bony proxies against masseter mass (left) and masseter physiological cross-sectional area (PCSA) (right), following phylogenetic adjustment. Both variables linearized and log-transformed prior to analysis. Black line = caniformia; gray line = feliformia; dashed line = whole sample

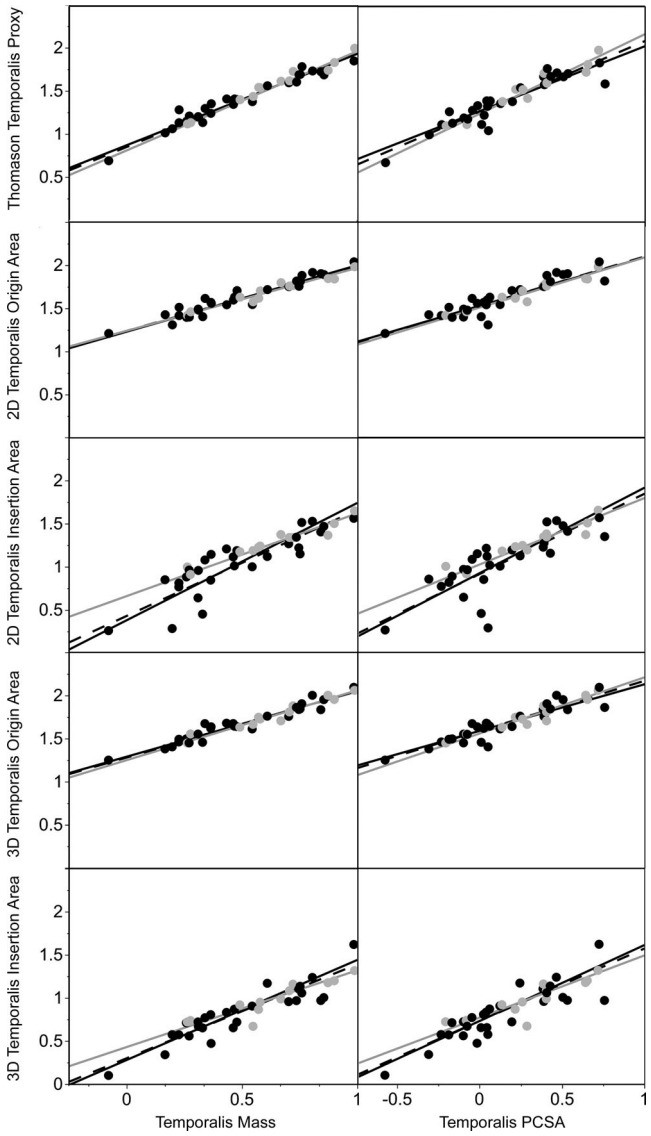

FIGURE 3 Reduced major axis (RMA) regressions of various bony proxies against temporalis mass (left) and temporalis physiological cross-sectional area (PCSA) (right), following phylogenetic adjustment. Both variables linearized and log-transformed prior to analysis. Black line = caniformia; gray line = feliformia; dashed line = whole sample

2.2 | Data analysis

Prior to all analyses, both myological and osteological data were first linearized (by reducing mass and area data to the ⅓ and ½ powers, respectively) and subsequently log-transformed. To assess the effects of phylogeny, conventional statistics were run using JMP15 Pro (SAS) and phylogenetically adjusted statistics were run using the R packages ape (Paradis & Schliep, 2019), phytools (Revell, 2012), geiger (Harmon et al., 2008), and nlme (Pinheiro et al., 2006). A phylogenetic branching sequence with dates was obtained from the 10kTrees Project (*Carnivora*: Version 1; Arnold et al., 2010). The parameter lambda (λ), which serves as a measure of phylogenetic signal, was estimated to examine the effect of phylogeny. To assess raw correlation between our myological data and each osteological predictor, reduced major axis (RMA) regressions were performed, independently for each muscle, and between each osteological variable and two muscle variables (muscle mass and PCSA). To account for the possible effects of phylogeny (see results), these analyses were repeated with phylogenetically adjusted RMA (pRMA) regressions. To account for the impact of body size upon raw values, each individual bony and myological variable was regressed using: (1) an ordinary

least squares (OLS) against body mass data derived from Wilson and Mittermeier (2009), and (2) a phylogenetic generalized least squared (PGLS) regression, again versus body mass data derived from Wilson and Mittermeier (2009). A second series of RMA regressions in which bony predictors were regressed against myological variables were then performed upon the residuals of these regressions (as per Perry et al., 2015) to calculate body-size adjusted relationships on both the original and phylogenetically adjusted datasets.

3 | RESULTS

3.1 | Test for phylogenetic significance

Estimates of the parameter lambda (λ), which serves as a measure of phylogenetic signal, indicate that the topology and branch lengths of the phylogenetic tree utilized account for some of the variation in osteological correlates of the masseter and temporalis relative to both muscle mass and PCSA. As such, only summary statistics and figures using phylogenetically adjusted regressions are reported and discussed in text hereafter. Summary statistics and figures for conventional regressions are included as supplementary online materials (Tables S1–S4, Figures S1–S6).

3.2 | Methodological comparisons

Regression of all raw osteological estimates against muscle masses produced universally strong agreement (r^2 = .75–.91), as expected due to the wide distribution of body masses across our sample and the close relationship between body mass, muscle mass, and cranial size across the order Carnivora (Table 2; Figures 2 and 3). Regression of raw bony metrics against PCSA yielded similar, though slightly reduced, correlations (r^2 = .65–.84; Table 3), in line with Prediction 4.

When accounting for body mass, however, significant variance between bony predictors was observed (Tables 4 and 5; Figures 4 and 5). For both, the masseter and the temporalis, Thomason "dry skull" technique yielded the strongest correlations with muscle mass (r^2 = .63 and .51, respectively). When considering PCSA, the "dry skull" technique (r^2 = .27 and .18 for the masseter and temporalis, respectively) yielded relatively similar results to the 3D-origin areas (r^2 = .32 and .09, respectively). Thus, prediction 1 was largely unsupported. When comparing techniques using muscle attachment areas, most masseteric proxies (3D-masseter origin, 3D-masseter insertion, and both 2D-masseter insertion proxies) produced similar results when predicting muscle mass (r^2 = .54–.56). However, masseter 2D-origin was notably less predictive of muscle mass (r^2 = .14). The same trends were also observed when predicting PCSA (Table 5). For the temporalis, 3D-origin area was more strongly correlated with mass and PCSA (r^2 = .30 and .09, respectively) than any other attachment area metric. Temporalis 2D-origin area and 3D-insertion area yielded similar results for both mass and PCSA, while 2D-insertion area (r^2 = .03 and .01 for mass and PCSA, respectively) was consistently the least predictive metric. Thus, Prediction 2 was partially supported. Finally, muscle attachment areas associated with a broad fibrous enthesis (as opposed to a tendinous attachment) were consistently better predicted than tendinous insertion areas, using both 2D- and 3D-techniques. Thus, Prediction 3 was supported.

3.3 | Taxonomic variability

To more closely assess trends herein, data were subsequently separated and analyzed individually between the suborders Feliformia (families Felidae, Hyenidae, and Herpestidae) and Caniformia (families Canidae, Ursidae, Mustelidae, Mephitidae, and Procyonidae). As with the order as a whole, raw osteological predictors were all closely

TABLE 3 Summary statistics following phylogenetic reduced major axis (RMA) regressions of bony correlate predictors against physiological cross-sectional area (PCSA)

	Bony metric	Slope All carnivores	Intercept	R^2	Slope Caniformia	Intercept	R^2	Slope Feliformia	Intercept	R^2
Masseter	Thomason "dry skull"	0.77	1.49	.84**	0.77	1.51	.79**	0.76	1.49	.94**
	2D origin	0.13	1.02	.80**	0.14	1.03	.77**	0.11	1.01	.93**
	2D insertion (SM + DM)	0.87	0.94	.68	0.98	0.99	.71	0.66	0.95	.74*
	2D insertion (SM,DM,ZM)	0.86	1.36	.81*	0.86	1.39	.76	0.91	1.30	.98
	3D origin	0.99	0.94	.68	1.08	0.96	.67	0.77	1.00	.83
	3D insertion (SM,DM,ZM)	0.81	1.38	.82**	0.77	1.40	.75*	0.90	1.33	.96
Temporalis	Thomason "dry skull"	0.82	1.28	.82**	0.75	1.29	.80	0.92	1.26	.93
	2D origin	0.57	1.53	.82**	0.56	1.53	.81**	0.58	1.51	.92**
	2D insertion	0.93	0.91	.65	0.99	0.92	.58	0.77	1.02	.88*
	3D origin	0.58	1.59	.80**	0.54	1.59	.79**	0.65	1.56	.91**
	3D insertion	0.84	0.73	.69	0.88	0.73	.70	0.72	0.77	.59

Note: Statistical significance is indicated by *p < .05 and **p < .01.

TABLE 4 Summary statistics following reduced major axis (RMA) regressions of body-mass and phylogenetically adjusted residuals of bony predictors against muscle mass

	Masseter r^2 following BM and phylogenetic correction				Temporalis r^2 following BM and phylogenetic correction		
Bony metric	All carnivores	Caniformia	Feliformia	Bony metric	All carnivores	Caniformia	Feliformia
Thomason "dry skull"	.63 **	.63 **	.21	Thomason "dry skull"	.51 **	.52 **	.55 **
2D origin	.14	.23 **	.20	2D origin	.22 **	.22 *	.40 *
2D insertion (SM + DM)	.54 **	.47 **	.52 **	2D insertion	.03	.00	.34 *
2D insertion (SM,DM,ZM)	.56 **	.59 **	.21				
3D origin	.54 **	.42 **	.12	3D origin	.30 **	.26 **	.55 **
3D insertion	.54 **	.64 **	.21	3D insertion	.20 **	.16 *	.32

Note: Statistical significance is indicated by *$p < .05$ and **$p < .01$.

TABLE 5 Summary statistics following reduced major axis (RMA) regressions of body-mass and phylogenetically adjusted residuals of bony predictors against physiological cross-sectional area (PCSA)

	Masseter r^2 following BM and phylogenetic correction				Temporalis r^2 following BM and phylogenetic correction		
Bony metric	All carnivores	Caniformia	Feliformia	Bony metric	All carnivores	Caniformia	Feliformia
Thomason "dry skull"	.27 **	.14 *	.44 *	Thomason "dry skull"	.18 **	.15 *	.15
2D origin	.02 *	.06	.27	2D origin	.06 *	.05	.24
2D insertion (SM + DM)	.26 **	.21 *	.45 *	2D insertion	.01	.03	.06
2D insertion (SM,DM,ZM)	.27 **	.17 *	.36 *				
3D origin	.32 **	.19 *	.27	3D origin	.09	.05	.32
3D insertion	.26 **	.16 *	.55 **	3D insertion	.05	.04	.04

Note: Statistical significance is indicated by *$p < .05$ and **$p < .01$.

correlated with muscle mass due to the strong effects of body size. However, when accounting for body mass, a strong discrepancy between suborders was observed.

Within the masseter, similar trends were observed between Caniforms and Feliforms, with a slight tendency towards stronger correlations between osteology and myology in the Caniform suborder (Figure 6; Tables 4 and 5). By contrast, the temporalis in Feliforms was *notably better* predicted using osteological metrics than in caniforms, particularly when analyzing attachment area proxies (Figure 7; Tables 4 and 5). Thus, Prediction 5 was partially supported.

4 | DISCUSSION

4.1 | Evaluating bony predictors of muscle size

Analysis of several common bony predictors of muscle size yielded vastly differing results. Firstly, despite recent reports highlighting the limitations of the "dry skull" technique in certain lineages, this method proved most predictive of all those evaluated here (Tables 4 and 5). Though relatively simple, that is, relying on two photographs taken in consistent planes, it appears that this method, initially developed and tested within carnivores (Thomason, 1991), remains the best technique for estimations of muscle mass and PCSA within this order. This finding is broadly supportive of the application of this approach in several studies attempting to osteologically predict patterns in bite force across diverse carnivoran samples (see Christiansen & Adolfssen, 2005; Christiansen & Wroe, 2007). While this finding was counter to Prediction 1, these results likely reflect the emphasis placed by this metric upon muscle *thickness*. Specifically, using photographs taken in a transverse plane, as opposed to the use of lateral cranial photographs, allows for the width of muscles to be accounted for (albeit indirectly) by incorporating the lateral flaring of the zygomatic arch into the estimation of muscle size. In so doing, this technique provides a more *volumetric* estimation than that provided by either 2D or 3D measurements of muscle attachment *areas*.

Given this, it can be inferred that as the masticatory muscles increase in mass (and therefore in volume), the attachment areas associated with the muscles themselves do not scale in proportion. This is demonstrated by analyzing the allometry of muscle attachment areas versus the muscles themselves; for example, temporalis mass (slope = 0.99, 95% CIs = 0.91–1.07) and PCSA (slope = 1.22, 95% CIs = 1.08–1.38) scale with (or approaching) positive allometry relative to body mass, yet the muscle's broad cranial attachment area scales with negative allometry relative to body mass (slope = 0.76,

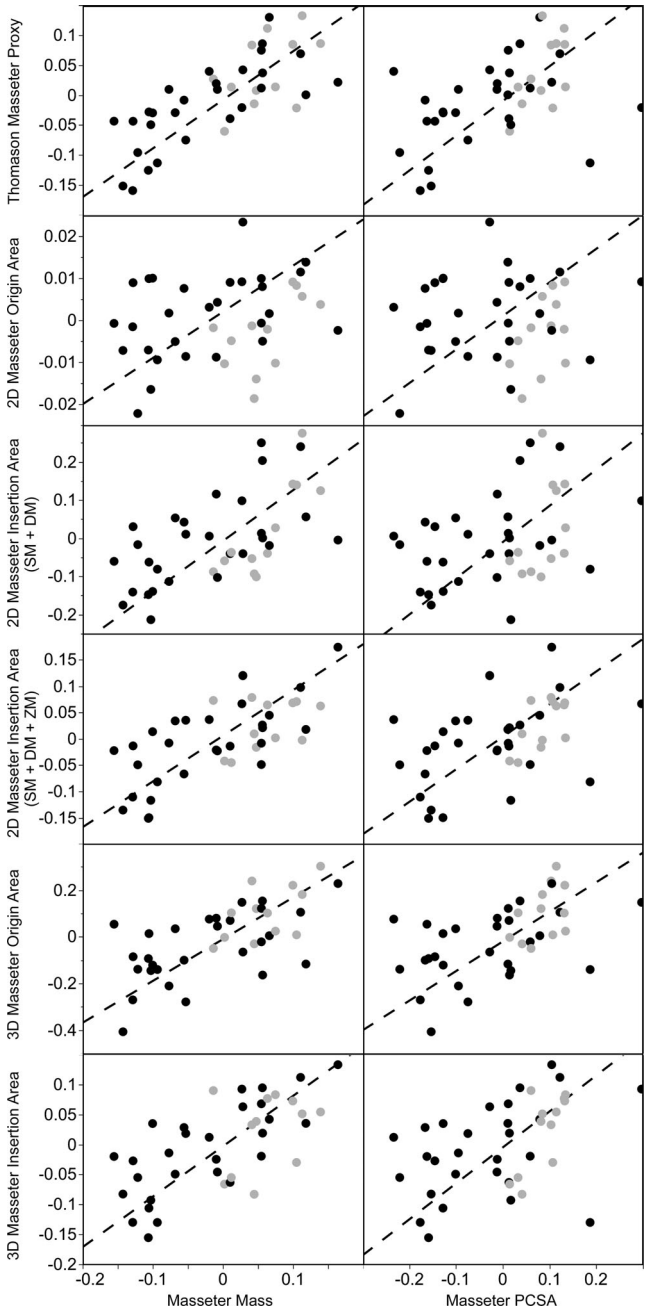

FIGURE 4 Phylogenetic generalized least squared (PGLS) regressions of residuals of bony proxies against masseter mass (left) and masseter PCSA (right), following adjustment for body mass. Black points = caniformia; gray points = feliformia

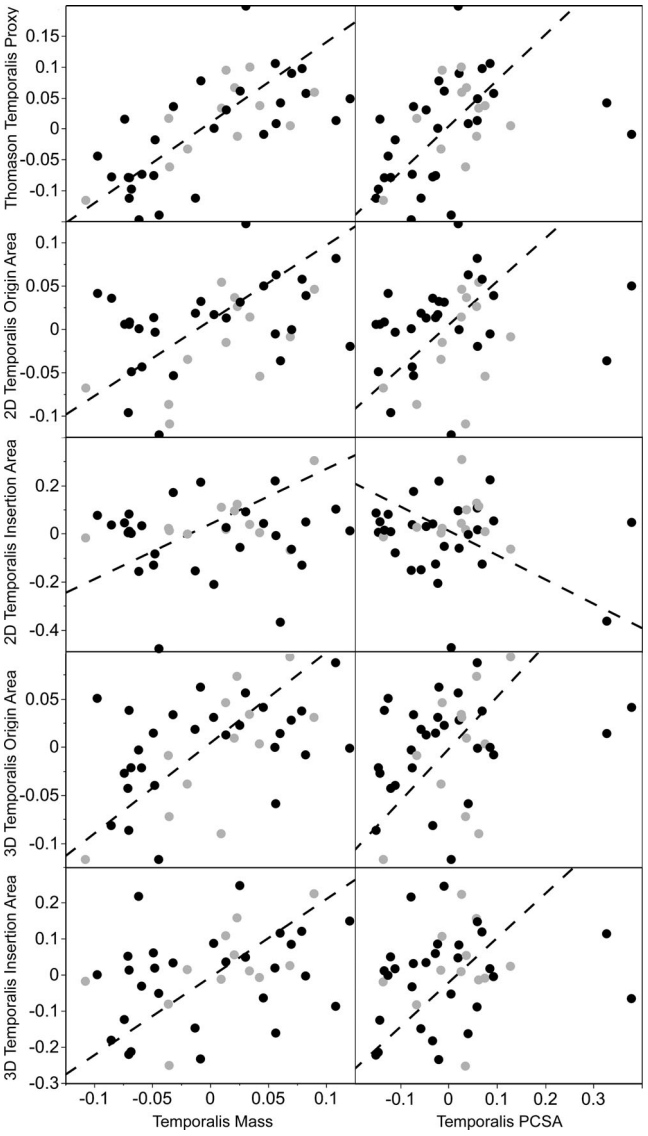

FIGURE 5 Phylogenetic generalized least squared (PGLS) regressions of residuals of bony proxies against temporalis mass (left) and temporalis PCSA (right), following adjustment for body mass. Black points = caniformia; gray points = feliformia

95% CIs = 0.69–0.83 for 2D area; slope = 0.78, 95% CIs = 0.71–0.85 for 3D area). This relationship contributes to the weak predictive relationship (most notably temporalis insertion, but also masseter origin) between the area occupied by the skeletal enthesis site and the size of the muscle itself. Instead, it would appear that an increase in muscle volume might be largely achieved by increasing muscle thickness, such that the larger muscles are better captured by metrics that estimate the muscle cross-section (such as the Thomason "dry skull" method) rather than those that estimate the dimensional areas of attachment sites.

This observation fits within a growing literature base that suggests attachment areas alone are potentially poor predictors of overall muscle size. The quantification of muscle attachment sites has been widely used to estimate muscle size and function in archeological populations, even serving as a basis from which to infer occupational intensity (Karakostis et al., 2017) or the practice of specific activities such as harpoon launching (Hawkey & Merbs, 1995). However, neither direct measurements of attachment size (e.g., see Hawkey & Merbs, 1995; Henderson, 2013; Henderson et al., 2013; Milella, 2014) nor calculations of optical complexity (Wallace et al., 2017; Zumwalt, 2006) are supported consistently by experimental studies (see Rabey et al., 2015; Turcotte et al., 2020; Wallace et al., 2017; Williams-Hatala et al., 2016; Zumwalt, 2006). For example, Rabey et al. (2015) demonstrated a clear division in the mass and internal architecture of the

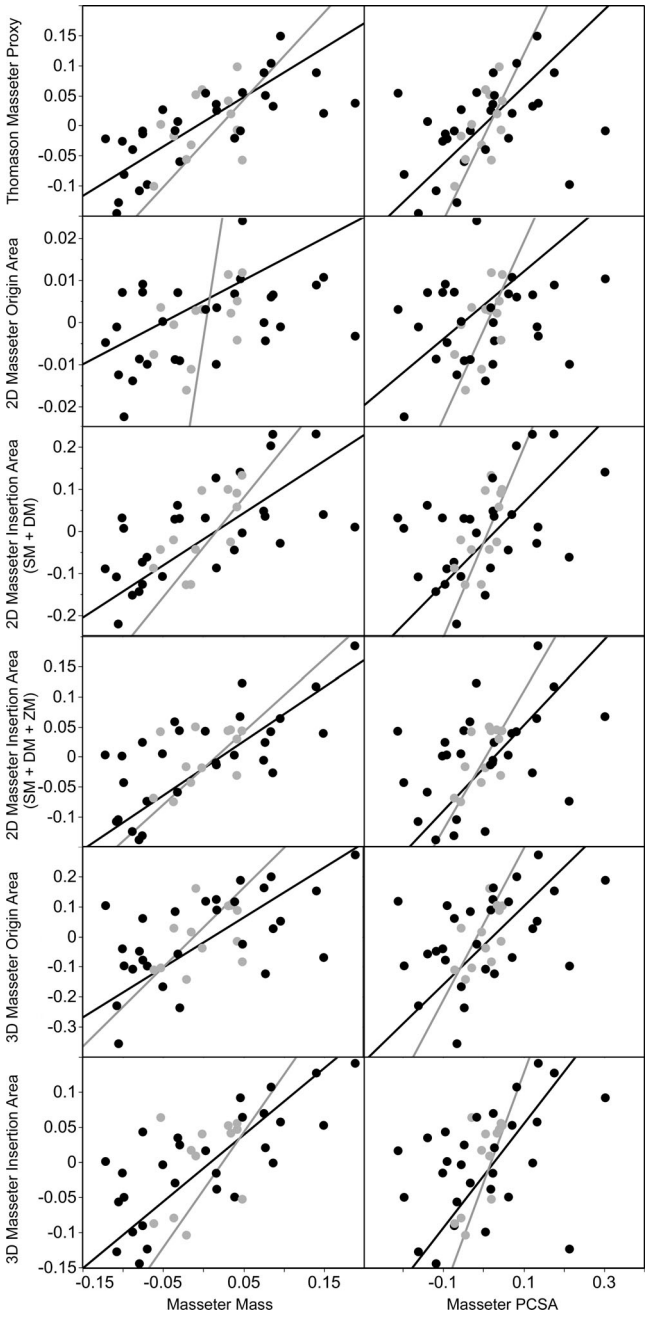

FIGURE 6 Reduced major axis (RMA) regressions of PGLS residuals of bony proxies against masseter mass (left) and masseter PCSA (right), followi6g adjustment for body mass. Black line and points = caniformia; gray line and points = feliformia

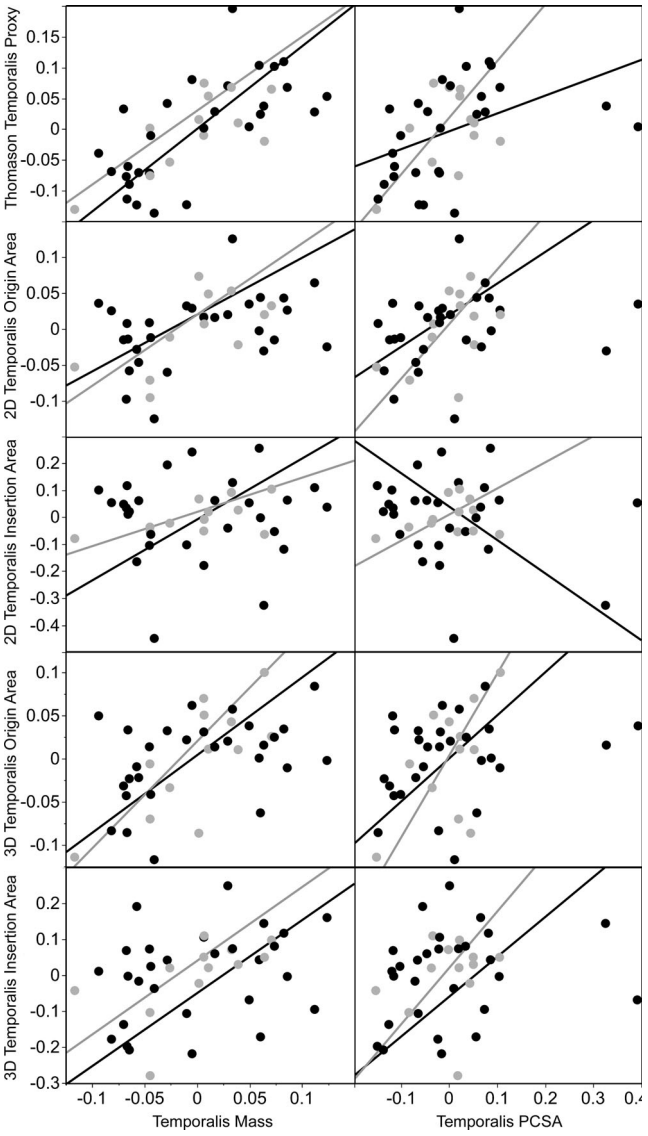

FIGURE 7 Reduced major axis (RMA) regressions of PGLS residuals of bony proxies against temporalis mass (left) and temporalis physiological cross-sectional area (PCSA) (right), following adjustment for body mass. Black line and points = caniformia; gray line and points = feliformia

three deltoideus muscles among three groups of exercised and control mice. However, the authors did not observe significant differences between the mouse groups in terms of muscle attachment morphology (i.e., 2D-linear measurements), indicating that muscle size and shape responded to exercise treatment in a way that the skeleton did not. Similar results are found in Zumwalt (2006) and Wallace et al. (2017), in which no relationship was found between 3D-surface area or complexity and exercise group in sheep and turkeys, respectively. Additionally, an analysis by Williams-Hatala et al. (2016) of cadaveric human hands showed no relationship between 3D-enthesis area and muscle weight in the first metacarpal and opponens pollicis ($r = .062$; $p = .802$).

Conversely, Rabey et al.'s (2015) analysis also included measurement of periosteal bone growth rate, which did differ significantly among the experimental groups ($p = <.001$). In the same mice, Turcotte et al. (in press) observed differences in cross-sectional geometry at the deltoid crest due to exercise regime. Additionally, studies of human archeological material have repeatedly demonstrated a relationship between 3D-enthesis area in the hand and living occupation, which has an assumed connection to muscle use and therefore size (Karakostis et al., 2017; Karakostis & Lorenzo, 2016). Similarly, morphometric analyses in suids have shown a relationship between muscle force potential (i.e., PCSA) and both the volume and

topography of cortical bone in the humerus and calcaneus (Harbers et al., 2020, Harbers et al., 2020). These conflicting observations suggest that, while measurements of attachment site length or surface area may fail to fully account for muscle size, other aspects of enthesis biology may provide fruitful indicators of myological properties.

4.2 | Muscle-specific trends in osteological estimates

In addition to appraising the above techniques for estimating muscle size within osteological samples, the data presented here also highlight several muscle-specific trends. Firstly, it was observed that the temporalis origin provided a stronger estimate of total temporalis mass than did the corresponding temporalis insertion when measured using 2D-surface areas (Table 4). This finding was not surprising, as the broad, fleshy origin of the temporalis muscle would intuitively seem a better approximation for the overall size of this muscle than would its smaller, tendinous insertion present on the coronoid process of the mandible. However, this discrepancy between attachment sites was not apparent when using 3D-surface scans to estimate attachment area (Table 4). This likely reflects the positioning of the temporalis insertion itself, which wraps fully around the anterior border of the coronoid process—much of which is obscured in a cranial lateral photograph but can be accessed and accounted for in 3D-data sets by rotating the specimen while isolating the attachment surface. Thus, when attachments alone must be used for estimates of muscle size, it would seem that 3D-approaches using surface data are potentially more predictive overall; though this technique appears inferior, at least among the Carnivora, to the "dry skull" technique.

It should also be noted that, in 2D-measurements of the insertion area within the masseteric complex, both the smaller SM + DM (superficial masseter and deep masseter) attachment area and the more expansive SM + DM + ZM (superficial masseter, deep masseter, and zygomaticomandibularis) area (Figure 1a, dark and dark+light blue respectively) were similarly correlated with muscle mass and PCSA (Tables 4 and 5). Thus, despite the insertion area of the zygomaticomandibularis (ZM) within the masseteric fossa being relatively large in proportion to the muscle itself, the inclusion of this additional attachment does not confound the relationship between muscle size and attachment area. Therefore, both techniques appear equally capable of estimating muscle mass and PCSA, though both remain less effective than volumetric estimates of muscle cross-sectional area.

4.3 | Taxonomic observations

While no strong differences between individual taxa or suborders were anticipated, a number of interesting observations should be noted. First, these data suggest that bony correlates (using all techniques considered herein) are universally more predictive of temporalis size and force within feliforms than in caniforms (Tables 4 and 5). This may reflect the increased variation in neurocranial shape within caniforms (e.g., the elongated neurocrania of many mustelids vs. the more rounded neurocrania of canids and ursids) versus a more uniform neurocranial shape across feliforms that largely varies in scale, as opposed to shape alone (Ewer, 1973; Radinsky, 1981a; Radinsky, 1981b).

It should also be noted that several species showed a consistently poor correlation between muscle size and several bony proxies. Mass and PCSA for both the temporalis and masseter were consistently overestimated in *Eira barbara*, *Tremarctos ornatus*, *Ursus americanus*, and *Vulpes macrotis*. Additionally, temporalis, but not masseter, mass and PCSA were overestimated by all osteological correlates in *Taxidea taxus*. At the other extreme, the mass and PCSA of both temporalis and masseter were most strongly underestimated in *Spilogale putorius* and *Mephitis mephitis*, the two mephitids within our sample—suggesting a difference in the shape of skunk skulls that confounds myological predictions relative to other carnivorans. The other taxa for which both size and force were consistently underestimated osteologically were *Helarctos malayanus* and *Leptailurus serval*. Temporalis, but not masseter, mass and PCSA were also overestimated by all osteological correlates in *Pteronura brasiliensis*; while the inverse was observed in *Canis rufus*.

4.4 | Methodological limitations

Bony correlates within the cranium and mandible have been used to estimate masticatory muscle size and contractile force potential across a huge variety of both extant and fossil taxa (e.g., Blanco et al., 2012; Demes & Creel, 1988; Grandal-d'Anglade, 2010; Meers, 2002; Perry et al., 2015; Wroe et al., 2005). Though the sample analyzed herein was selected to maximize both taxonomic number and morphological diversity within the order Carnivora, our findings may not translate well to other lineages. Indeed, as observed in Chiroptera by Davis et al. (2010), the "dry skull" method, which was originally validated using a carnivoran sample, does not work well for all other orders. Thus, caution should be exercised when applying any single method as a robust methodological predictor across diverse phylogenies.

Additionally, it should be noted that the quantification of muscle attachment areas (measured via either 2D- or 3D-techniques) is inherently reliant on the accurate and consistent visual discrimination of the boundaries of attachment sites. While in several cases these boundaries are clearly defined (e.g., the masseteric scar on the mandible, the temporal fossa on the cranium), other attachment sites (particularly the mandibular insertion of the temporalis) are less clear and may be more open to misidentification. Further, as empirical studies continue to caution against the predictive values of entheses as proxies for muscle properties such as mass and PCSA, care should be taken to guard against over-interpretation of diet, locomotion, or behavior on the basis of osteological estimates of muscle size and PCSA alone. Rather, such estimations should be combined with other ecological markers to enhance our understanding of ecology within understudied or extinct lineages.

5 | CONCLUSIONS

Overall, our findings indicate that volumetric approaches—including the "dry skull" technique outlined by Thomason (1991)—provide stronger approximations of muscle size and PCSA than entheseal approaches that utilize muscle attachment areas. This likely reflects the importance of accounting for muscle thickness in osteological estimations of the masticatory musculature. Acknowledging the comparative weakness of myological estimates derived from attachment areas may have important implications for palaeobiological reconstructions of muscle dimensions and force potential. Future studies are necessary, however, to evaluate such relationships across other mammalian lineages.

ACKNOWLEDGMENTS

We would like to thank the managing Editor and two anonymous reviewers for their contributions and suggestions toward refining this manuscript. We are also grateful to Melinda Franke, Nikole Worden, and Indya Thompson for their assistance with collecting data used in this study. Funding was provided by the National Sciences Foundation IOS-15-57125 and BCS-14-40599.

AUTHOR CONTRIBUTIONS

Edwin Dickinson: Conceptualization (equal); data curation (equal); formal analysis (lead); investigation (equal); methodology (lead); project administration (equal); resources (equal); software (equal); supervision (equal); validation (equal); visualization (equal); writing - original draft (lead); writing-review & editing (equal). **Jillian Davis:** Conceptualization (equal); data curation (equal); formal analysis (supporting); funding acquisition (equal); investigation (equal); methodology (equal); project administration (equal); resources (equal); supervision (equal); validation (supporting); writing - original draft (supporting). **Ashley Deutsch:** Formal analysis (equal); investigation (supporting); methodology (equal); writing - original draft (equal); writing-review & editing (equal). **Dhuru Patel:** Data curation (supporting); investigation (supporting); writing - original draft (supporting); writing-review & editing (supporting). **Akash Nijhawan:** Formal analysis (supporting); investigation (supporting); methodology (supporting); writing - original draft (supporting); writing-review & editing (supporting). **Meet Patel:** Investigation (supporting); methodology (supporting); writing - original draft (supporting); writing-review & editing (supporting). **Abby Blume:** Investigation (supporting); methodology (supporting); writing-review & editing (supporting). **Jordan Gannon:** Investigation (supporting); methodology (supporting); writing-review & editing (supporting). **Cassandra Turcotte:** Investigation (supporting); methodology (supporting); writing - original draft (supporting); writing-review & editing (supporting). **Christopher Walker:** Funding acquisition (supporting); investigation (supporting); project administration (supporting); resources (equal); software (equal); supervision (supporting); writing-review & editing (equal). **Adam Hartstone-Rose:** Conceptualization (equal); data curation (equal); formal analysis (equal); funding acquisition (lead); investigation (equal); methodology (equal); project administration (lead); resources (equal); software (equal); supervision (equal); validation (equal); visualization (equal); writing - original draft (equal); writing-review & editing (equal).

PEER REVIEW

The peer review history for this article is available at https://publons.com/publon/10.1002/jmor.21400.

DATA AVAILABILITY STATEMENT

Three-dimensional scans of all specimens are being archived in Morphosource. Any that are not yet accessible through that site and all other data that support the findings of this study are available from the corresponding author upon reasonable request.

ORCID

Adam Hartstone-Rose https://orcid.org/0000-0001-5307-5573

REFERENCES

Aguirre, L. F., Herrel, A., van Damme, R., & Matthysen, E. (2002). Ecomorphological analysis of trophic niche partitioning in a tropical savannah bat community. *Proceedings Biological sciences/The Royal Society*, *269*, 1271–1278.

Antón SC. 1994. *Masticatory muscle architecture and bone morphology in primates*. (PhD Dissertation). University of California Berkeley.

Antón, S. C. (1999). Macaque masseter muscle: Internal architecture, fiber length and cross-sectional area. *International Journal of Primatology*, *20*, 441–462.

Arnold, C., Matthews, L. J., & Nunn, C. L. (2010). The 10kTrees website: A new online resource for primate phylogeny. Version 1: Carnivora. *Evolutionary Anthropology*, *19*, 114–118.

Becerra, F., Echeverría, A., Vassallo, A. I., & Casinos, A. (2011). Bite force and jaw biomechanics in the subterranean rodent Talas tuco-tuco (Ctenomys talarum)(Caviomorpha: Octodontoidea). *Canadian Journal of Zoology*, *89*, 334–342.

Becerra, F., Echeverría, A. I., Casinos, A., & Vassallo, A. I. (2014). Another one bites the dust: Bite force and ecology in three caviomorph rodents (Rodentia, Hystricognathi). *Journal of Experimental Zoology Part A: Ecological Genetics and Physiology*, *321*, 220–232.

Binder, W. J., & Van Valkenburgh, B. (2000). Development of bite strength and feeding behaviour in juvenile spotted hyenas (*Crocuta crocuta*). *Journal of Zoology*, *252*(3), 273–283.

Blanco, R. E., Rinderknecht, A., & Lecuona, G. (2012). The bite force of the largest fossil rodent (Hystricognathi, Caviomorpha, Dinomyidae). *Lethaia*, *45*, 157–163.

Brassard, C., Merlin, M., Guintard, C., Monchâtre-Leroy, E., Barrat, J., Bausmayer, N., Bausmayer, S., Bausmayer, A., Beyer, M., Varlet, A., & Houssin, C. (2020). Bite force and its relationship to jaw shape in domestic dogs. *Journal of Experimental Biology*, *223*(16), 1–12.

Brassard, C., Merlin, M., Monchâtre-Leroy, E., Guintard, C., Barrat, J., Garès, H., Larralle, A., Triquet, R., Houssin, C., Callou, C., & Cornette, R. (2021). Masticatory system integration in a commensal canid: Interrelationships between bones, muscles and bite force in the red fox. *Journal of Experimental Biology*, *224*(5), jeb224394.

Christiansen, P., & Adolfssen, J. S. (2005). Bite forces, canine strength and skull allometry in carnivores (Mammalia, Carnivora). *Journal of Zoology*, *266*, 133–151.

Christiansen, P., & Wroe, S. (2007). Bite forces and evolutionary adaptations to feeding ecology in carnivores. *Ecology Letters*, *88*, 347–358.

Davis, J. L., Santana, S. E., Dumont, E. R., & Grosse, I. R. (2010). Predicting bite force in mammals: Two-dimensional versus three-dimensional lever models. *The Journal of Experimental Biology*, *213*, 1844–1851.

Dechow, P. C., & Carlson, D. S. (1990). Occlusal force and craniofacial biomechanics during growth in rhesus monkeys. *American Journal of Physical Anthropology*, *83*, 219–237.

Demes, B., & Creel, N. (1988). Bite force, diet, and cranial morphology of fossil hominids. *Journal of Human Evolution*, *17*, 657–670.

Deutsch, A. R., Dickinson, E., Leonard, K. C., Pastor, F., Muchlinski, M. N., & Hartstone-Rose, A. (2020). Scaling of anatomically derived maximal bite force in primates. *The Anatomical Record*, *303*, 2026–2035.

Dumont, E., Herrel, A., Medellin, R., Vargas-Contreras, J., & Santana, S. (2009). Built to bite: Cranial design and function in the wrinkle-faced bat. *Journal of Zoology*, *279*, 329–337.

Emerson, S. B., & Radinsky, L. (1980). Functional analysis of Sabertooth cranial morphology. *Paleobiology*, *6*, 295–312.

Ewer, R. F. (1973). *The carnivores*. Cornell University Press.

Fabre, A. C., Perry, J. M., Hartstone-Rose, A., Lowie, A., Boens, A., & Dumont, M. (2018). Do muscles constrain skull shape evolution in Strepsirrhines? *The Anatomical Record*, *301*(2), 291–310.

Forbes-Harper, J., Crawford, H., Dundas, S., Warburton, N., Adams, P., Bateman, P., Calver, M., & Fleming, P. (2017). Diet and bite force in red foxes: Ontogenetic and sex differences in an invasive carnivore. *Journal of Zoology*, *303*, 54–63.

Gans, C. (1982). Fiber architecture and muscle function. *Exercise and Sport Sciences Reviews*, *10*, 160–207.

Gans, C., & Bock, W. J. (1965). The functional significance of muscle architecture - a theoretical analysis. *Ergebnisse der Anatomie und Entwicklungsgeschichte*, *38*, 115–142.

Grandal-d'Anglade, A. (2010). Bite force of the extinct Pleistocene cave bear *Ursus spelaeus* Rosenmüller from Europe. *Comptes Rendus Palevol*, *9*, 31–37.

Gröning, F., Jones, M. E., Curtis, N., Herrel, A., O'Higgins, P., Evans, S. E., & Fagan, M. J. (2013). The importance of accurate muscle modelling for biomechanical analyses: A case study with a lizard skull. *Journal of the Royal Society Interface*, *10*(84), 20130216.

Harbers, H., Neaux, D., Ortiz, K., Blanc, B., Laurens, F., Baly, I., Callou, C., Schafberg, R., Haruda, A., Lecompte, F., Casabianca, F., Studeur, J., Renaud, S., Cornette, R., Locatelli, U., Vigne, J.-D., Herrel, A., & Cucchi, T. (2020). The mark of captivity: Plastic responses in the ankle bone of a wild ungulate (*Sus scrofa*). *Royal Society Open Science*, *7*(3), 192039.

Harbers, H., Zanolli, C., Cazenave, M., Theil, J. C., Ortiz, K., Blanc, B., Locatelli, Y., Schafberg, R., Lecompte, F., Baly, I., Laurens, F., Callou, C., Vigne, J.-D., Herrel, A., Puymerail, L., & Cucchi, T. (2020). Investigating the impact of captivity and domestication on limb bone cortical morphology: An experimental approach using a wild boar model. *Scientific Reports*, *10*(1), 1–13.

Harmon, L. J., Weir, J. T., Brock, C. D., Glor, R. E., & Challenger, W. (2008). GEIGER: Investigating evolutionary radiations. *Bioinformatics*, *24*(1), 129–131.

Hartstone-Rose, A., Dickinson, E., Worden, N., Deutsch, A., & Hirschkorn, G. (in press). Masticatory muscle architectural correlates of dietary diversity in Canidae, Ursidae, and across the order Carnivora. *The Anatomical Record*.

Hartstone-Rose, A., Hertzig, I., & Dickinson, E. (2019). Bite force and masticatory muscle architecture adaptations in the dietarily diverse Musteloidea (Carnivora). *The Anatomical Record*, *302*, 2287–2299.

Hartstone-Rose, A., Perry, J. M., & Morrow, C. J. (2012). Bite force estimation and the fiber architecture of felid masticatory muscles. *The Anatomical Record*, *295*, 1336–1351.

Hawkey, D. E., & Merbs, C. F. (1995). Activity-induced musculoskeletal stress markers (MSM) and subsistence strategy changes among ancient Hudson Bay Eskimos. *International Journal of Osteoarchaeology*, *5*, 324–338.

Henderson, C. (2013). Do diseases cause entheseal changes at fibrous entheses? *International journal of Paleopathology*, *3*, 64–69.

Henderson, C. Y., Mariotti, V., Pany-Kucera, D., Villotte, S., & Wilczak, C. (2013). Recording specific entheseal changes of fibrocartilaginous entheses: Initial tests using the Coimbra method. *International Journal of Osteoarchaeology*, *23*, 152–162.

Herrel, A., Damme, R. V., Vanhooydonck, B., & Vree, F. D. (2001). The implications of bite performance for diet in two species of lacertid lizards. *Canadian Journal of Zoology*, *79*(4), 662–670.

Herrel, A., De Grauw, E. D., & Lemos-Espinal, J. A. (2001). Head shape and bite performance in xenosaurid lizards. *Journal of Experimental Zoology*, *290*(2), 101–107.

Herrel, A., & O'Reilly, J. C. (2006). Ontogenetic scaling of bite force in lizards and turtles. *Physiological and Biochemical Zoology*, *79*(1), 31–42.

Karakostis, F. A., Hotz, G., Scherf, H., Wahl, J., & Harvati, K. (2017). Occupational manual activity is reflected on the patterns among hand entheses. *American Journal of Physical Anthropology*, *164*, 30–40.

Karakostis, F. A., & Lorenzo, C. (2016). Morphometric patterns among the 3D surface areas of human hand entheses. *American Journal of Physical Anthropology*, *160*, 694–707.

Law, C. J., Duran, E., Hung, N., Richards, E., Santillan, I., & Mehta, R. S. (2018). Effects of diet on cranial morphology and biting ability in musteloid mammals. *Journal of Evolutionary Biology*, *31*, 1918–1931.

Leonard KC, Worden N, Boettcher ML, Dickinson E, Hartstone-Rose A. (2021). Effects of long-term ethanol storage on muscle architecture. *The Anatomical Record*, *2021*, 1–12.

Leonard, K. C., Worden, N., Boettcher, M. L., Dickinson, E., Omstead, K. M., Burrows, A. M., & Hartstone-Rose, A. (2021). Anatomical and ontogenetic influences on muscle density. *Scientific Reports*, *11*, 1–11.

Lieber, R. L. (1986). Skeletal muscle adaptability. I: Review of basic properties. *Developmental Medicine and Child Neurology*, *28*, 390–397.

Lieber, R. L., & Fridén, J. (2000). Functional and clinical significance of skeletal muscle architecture. *Muscle & Nerve*, *23*, 1647–1666.

Meers, M. B. (2002). Maximum bite force and prey size of tyrannosaurus rex and their relationships to the inference of feeding behavior. *Historical Biology*, *16*, 1–12.

Meyers, J. J., Herrel, A., & Birch, J. (2002). Scaling of morphology, bite force and feeding kinematics in an Iguanian and a Scleroglossian lizard. In P. Aerts, K. D'Août, A. Herrel, & R. Van Damme (Eds.), *Topics in functional and ecological vertebrate morphology* (pp. 47–62). Shaker Publishing.

Milella, M. (2014). The influence of life history and sexual dimorphism on entheseal changes in modern humans and African great apes. *PLoS One*, *9*, e107963.

Nowak, R. M. (1991). *Walker's mammals of the world* (5th ed.). Johns Hopkins UP.

Paradis, E., & Schliep, K. (2019). Ape 5.0: An environment for modern phylogenetics and evolutionary analyses in R. *Bioinformatics*, *35*(3), 526–528.

Penrose, F., Cox, P., Kemp, G., & Jeffery, N. (2020). Functional morphology of the jaw adductor muscles in the Canidae. *The Anatomical Record*, *303*, 2878–2903.

Perry, J. M. G., St Clair, E. M., & Hartstone-Rose, A. (2015). Craniomandibular signals of diet in adapids. *American Journal of Physical Anthropology*, *158*, 646–662.

Pinheiro, J., Bates, D., DebRoy, S., Sarkar, D., & Team, R. C. (2006). Nlme: Linear and nonlinear mixed effects models, *3*(4), 109.

Powell, P. L., Roy, R. R., Kanim, P., Bello, M. A., & Edgerton, V. R. (1984). Predictability of skeletal muscle tension from architectural determinations in Guinea pig hindlimbs. *Journal of Applied Physiology*, *57*, 1715–1721.

Rabey, K. N., Green, D. J., Taylor, A. B., Begun, D. R., Richmond, B. G., & McFarlin, S. C. (2015). Locomotor activity influences muscle architecture and bone growth but not muscle attachment site morphology. *Journal of Human Evolution*, *78*, 91–102.

Radinsky, L. B. (1981a). Evolution of skull shape in carnivores, 1: Representative modern carnivores. *Biological Journal of the Linnean Society*, *15*, 369–388.

Radinsky, L. B. (1981b). Evolution of skull shape in carnivores, 2: Additional modern carnivores. *Biological Journal of the Linnaean Society*, *16*, 337–355.

Rayne, J., & Crawford, G. N. C. (1972). The relationship between fibre length, muscle excursion and jaw movement in the rat. *Archives of Oral Biology*, *17*, 859–872.

Revell, L. J. (2012). Phytools: An R package for phylogenetic comparative biology (and other things). *Methods in Ecology and Evolution*, *3*(2), 217–223.

Ross, C. F., Porro, L. B., Herrel, A., Evans, S. E., & Fagan, J. F. (2018). Bite force and cranial bone strain in four species of lizards. *Journal of Experimental Biology*, *221*(23), jeb180240.

Santana, S., & Dumont, E. (2009). Connecting behaviour and performance: The evolution of biting behaviour and bite performance in bats. *Journal of Evolutionary Biology*, *22*, 2131–2145.

Schneider, C. A., Rasband, W. S., & Eliceiri, K. W. (2012). NIH image to ImageJ: 25 years of image analysis. *Nature Methods*, *9*, 671–675.

Thomason, J. J. (1991). Cranial strength in relation to estimated biting forces in some mammals. *Canadian Journal of Zoology-Revue Canadienne De Zoologie*, *69*, 2326–2333.

Turcotte, C., Rabey, K., Green, D., & McFarlin, S. (in press). Muscle attachment sites and behavioral reconstruction: An experimental test of muscle-bone structural response to habitual activity. *American Journal of Physical Anthropology*.

Turcotte, C. M., Green, D. J., Kupczik, K., McFarlin, S., & Schulz-Kornas, E. (2020). Elevated activity levels do not influence extrinsic fiber attachment morphology on the surface of muscle-attachment sites. *Journal of Anatomy*, *236*, 827–839.

Wallace, I. J., Winchester, J. M., Su, A., Boyer, D. M., & Konow, N. (2017). Physical activity alters limb bone structure but not entheseal morphology. *Journal of Human Evolution*, *107*, 14–18.

Williams, S. H., Peiffer, E., & Ford, S. (2009). Gape and bite force in the rodents *Onychomys leucogaster* and *Peromyscus maniculatus*: Does jaw-muscle anatomy predict performance? *Journal of Morphology*, *270*, 1338–1347.

Williams-Hatala, E., Hatala, K., Hiles, S., & Rabey, K. (2016). Morphology of muscle attachment sites in the modern human hand does not reflect muscle architecture. *Scientific Reports*, *6*, 28353.

Wilson, D. E., & Mittermeier, R. A. (2009). *Handbook of the mammals of the world Vol 1: Carnivores*. Lynx Edicions.

Wroe, S., McHenry, C., & Thomason, J. (2005). Bite club: Comparative bite force in big biting mammals and the prediction of predatory behaviour in fossil taxa. *Proceedings of the Royal Society B: Biological Sciences*, *272*, 619–625.

Zumwalt, A. (2006). The effect of endurance exercise on the morphology of muscle attachment sites. *Journal of Experimental Biology*, *209*, 444–454.

SUPPORTING INFORMATION

Additional supporting information may be found online in the Supporting Information section at the end of this article.

How to cite this article: Dickinson, E., Davis, J. S., Deutsch, A. R., Patel, D., Nijhawan, A., Patel, M., Blume, A., Gannon, J. L., Turcotte, C. M., Walker, C. S., & Hartstone-Rose, A. (2021). Evaluating bony predictors of bite force across the order Carnivora. *Journal of Morphology*, *282*(10), 1499–1513. https://doi.org/10.1002/jmor.21400